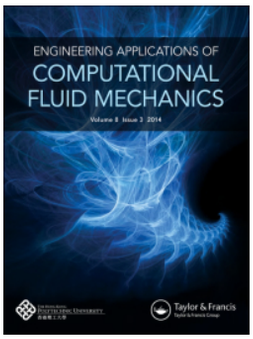

Taylor & Francis
Taylor & Francis Group

Engineering Applications of Computational Fluid Mechanics

ISSN: (Print) (Online) Journal homepage: www.tandfonline.com/journals/tcfm20

Discrete air model for large scale rapid filling process contained entrapped air

Rui-Lin Feng, Ling Zhou, Mohsen Besharat, ZiJian Xue, YunJie Li, QianXun Chen, YinYing Hu & YanQing Lu

To cite this article: Rui-Lin Feng, Ling Zhou, Mohsen Besharat, ZiJian Xue, YunJie Li, QianXun Chen, YinYing Hu & YanQing Lu (2024) Discrete air model for large scale rapid filling process contained entrapped air, Engineering Applications of Computational Fluid Mechanics, 18:1, 2428423, DOI: 10.1080/19942060.2024.2428423

To link to this article: https://doi.org/10.1080/19942060.2024.2428423

Published online: 15 Nov 2024.

ENGINEERING APPLICATIONS OF COMPUTATIONAL FLUID MECHANICS
2024, VOL. 18, NO. 1, 2428423
https://doi.org/10.1080/19942060.2024.2428423

Discrete air model for large scale rapid filling process contained entrapped air

Rui-Lin Feng[a], Ling Zhou[a,b], Mohsen Besharat[c], ZiJian Xue[d], YunJie Li[a], QianXun Chen[a], YinYing Hu[a] and YanQing Lu[a]

[a]College of Water Conservancy and Hydropower Engineering, Hohai University, Nanjing, People's Republic of China; [b]Yangtze Institute for Conservation and Development, Hohai University, Nanjing, People's Republic of China; [c]School of Civil Engineering, University of Leeds, Leeds, United Kingdom; [d]Department of Civil and Environmental Engineering, The Hong Kong Polytechnic University, Hong Kong, People's Republic of China

ABSTRACT

In this paper, a discrete air model (DAM) is developed to capture the discontinuous characteristics of air at different locations during the rapid filling process in long-range, large-scale water pipeline. By introducing the continuity and momentum equations of air and combining them with the water control equation and the interface continuity equation, an improved model based on the uniform air is derived. The accuracy of the model is verified by comparing it with experimental data and the results of the original uniform air model (UAM). Subsequently, a long-range, large-scale pipeline was considered to investigate the dynamic properties of air in large systems, which had not been covered in previous studies. Additionally, the influence of air dynamic characteristics on initial air volume affected by different air lengths and various pipe diameters in large systems – is further studied. Results show that an increased pipe diameter expands the contact area of the air–water interface, often resulting in the UAM underestimating the maximum peak pressure. The propagation process of transient waves in air is divided into three stages: propagation stage with multiple variation, maximum value stage with interface propulsive, and stability stage with several fluctuations, which corresponds to the pressure fluctuation curve. This explains the occurrence of small fluctuations and peaks in the curve. Therefore, the peak pressure simulated by the proposed DAM offers a better understanding of wave behaviours.

ARTICLE HISTORY
Received 19 August 2024
Accepted 6 November 2024

KEYWORDS
1D numerical modelling; discrete air; air-water interface; large-scale; rapid filling

1. Introduction

The development of a comprehensive water system is critical to address the uneven distribution of water resources and to boosting the nation's economic growth (Mariño & Loaiciga, 1985). The extended length and intricate design of the long-distance water transmission system present unique challenges (**Ling** Besharat et al., 2018; Vasconcelos et al., 2015; Zhou et al., 2011, 2024). The pipeline undergoes changes in operating conditions, water filling and discharging procedures during maintenance and repair, potentially inducing complex air–water two-phase flow and trapping substantial air (Bucur et al., 2017; Hatcher & Vasconcelos, 2017; Hu et al., 2024; Tasca et al., 2023). In 1982, a severe pressure surge in several North American cities was attributed to air entrapment, causing a sudden shift from gravity flow to pressure flow (Hamam & McCorquodale, 1982). These shifts often result in adverse transients, generating excessive hydraulic forces that stress pipeline infrastructure. Similarly, extensive basement and street flooding in Edmonton in 1995 caused significant facility damage due to air entrainment and release (City of Edmonton, 1995). Air presence can either mitigate pressure waves or cause extreme destructive pressure leading to catastrophic pipe blowouts or facility damage. The dynamic nature of air in water systems, particularly during rapid filling processes, poses significant challenges for hydraulic engineers. Air can become entrapped at multiple locations along a pipeline, where it interacts discontinuously with the water, creating complex pressure dynamics that are not easily captured by conventional models. In response to these challenges, advancements in discrete air modelling provide a more accurate depiction of air behaviour, addressing the limitations of uniform air assumptions that often underestimate peak pressures. These insights are critical for both the design and operation of large-scale water systems, where accurate prediction of pressure surges and air behaviour is essential to prevent infrastructure damage and ensure operational safety. The developed model provides engineers with

CONTACT Ling Zhou zlhhu@163.com College of Water Conservancy and Hydropower Engineering, Hohai University, Nanjing, Jiangsu, People's Republic of China; Yangtze Institute for Conservation and Development, Hohai University, Nanjing, Jiangsu, People's Republic of China

a better understanding of transient wave propagation, dividing it into three distinct stages and offering a more detailed explanation for the pressure fluctuation patterns observed during rapid filling.

Previous publications have explored the rapid water filling process through analytical solutions (Urbanowicz et al., 2023) and numerical simulations (Fuertes-Miquel et al., 2019). So far, numerous studies have focused on one-dimensional numerical simulation of pipe filling process (Lu et al., 2024; Xue et al., 2023). The one-dimensional models simulating the problem of rapid filling pipeline are generally divided into two categories: the first type applies the equations of pressurized flow and open flow respectively to different flow regions, known as interface tracking mixed flow models; the second type uses a single set of equations to simulate the pressurization effect in the flow region. The rigid water column model is a classical single set of equations model first proposed by Martin (1976). After continuous improvement by many scholars, considerations gradually expanded to include water elasticity, changes in water column length, and both steady and unsteady friction in pipelines (Coronado-Hernández et al., 2018; Hou et al., 2020). Fuertes et al. (2000) simulated the pressure change of the air pocket at the high point of an undulating pipeline based on the rigid water column model. Malekpour and Karney (2011) verified the stability of rigid water column model to simulate water filling process. The results demonstrated that the rigid water models exhibit limitations for cases involving long distances and small air volumes. Wylie et al. (1993) established the corresponding elastic water model and Zhou et al. (2013) successfully applied it to the movement containing multiple retained air pockets.

The shock capture model based on the mass and momentum equations of free-surface flow also simulates pressurization effects using a single set of equations. Vasconcelos and Marwell (2011) proposed the Two-component Pressure Approach (TPA) method to solve velocity changes caused by sub-atmospheric pressurized flows, which extended the applicability of the Saint-Venant equation in the case of air contained pressurized flow. Ferreira et al. (2024) successfully integrated the ideal air state equation into SWMM hydraulic software to simulate rapid filling while addressing the problem that the model cannot deal with the air pressurization in the filling process.

The above models tend to ignore the properties of the gas or adopt uniform air assumptions. The lack of consideration of gas space discretization cannot fully reflect the dynamic characteristics of gas compression and expansion, which is the knowledge gap in the existing models. Chaiko and Brinckman (2002) showed the deficiency of the uniform air model (UAM) when capturing interfacial pressure reflection at high pressure condition. The improved shock capture model (Trindade & Vasconcelos, 2011; Vasconcelos & Trindade, 2011, 2015), accounting for air phase pressure gradient in short pipe, does better in simulating the air–water interaction. Nonetheless, the previous research has the following limitations: (1) the model based on the rigid column model lacks the accurate representation for long-distance pipelines because it omits the water elasticity; (2) insufficient attention has been given to the wave propagation effect of air pocket in small-scale pipelines, neglecting the impact of scale.

The aim of this paper is to establish an elastic water column filling model considering discrete air effects. At the same time, the influence of discrete air under different pipe scales is quantitatively analyzed. Then the propagation mechanism of a transient wave in a water-filled pipe with the air dispersion effect is thoroughly investigated. The governing equations of air are introduced and combined with the water control equation and the interface continuity equation during the rapid filling process to derive the proposed discrete air model (DAM). Thereafter, the correctness of the model is verified by both laboratory experiments and UAM. In particular, research is conducted on the importance of air pressure waves in large-scale and long-distance water transport systems. Based on this, the air ratio in large-scale pipelines, pipe diameter, etc., are systematically analyzed and discussed to increase the basic understanding of the effects of two-phase flow transients. Finally, the main conclusions are drawn.

2. Mathematical model

This section aims to establish a comprehensive mathematical model for discrete air by developing more detailed air continuity and momentum equations, which are incorporated with the water control equations, pressure balance equations and the continuity equation at the air–water interface. This model is predicated on the following assumptions: (1) the air–water interface is perpendicular to the centreline of the pipeline; (2) the dissolution of air in water is neglected; and (3) a rigid pipeline connection is assumed, excluding fluid-structure interaction.

The continuity and momentum equations of the filling water region can be written as follows, which are consistent with the formulas used in Zhou et al. (2023).

$$\frac{\partial H_w}{\partial t} + \frac{{a_w}^2}{g}\frac{\partial V_w}{\partial x} = 0 \tag{1}$$

$$\frac{\partial H_w}{\partial x} + \frac{1}{g}\frac{\partial V_w}{\partial t} + J_Q + J_U = 0 \tag{2}$$

where, the subscript w represents water; H_w is the piezometric head; a_w is the wave speed; g is the acceleration of gravity; V_w is the average flow velocity; x is the distance along the pipe; t is time; J_Q and J_U represent the loss terms due to steady and unsteady friction, respectively.

The continuity and momentum equations for air can be written as:

$$\frac{\partial \rho_g}{\partial t} + \frac{\partial (\rho_g u_g)}{\partial x} = 0 \tag{3}$$

$$\frac{\partial (\rho_g u_g)}{\partial t} + \frac{\partial (\rho_g {u_g}^2 + P_g)}{\partial x} = 0 \tag{4}$$

where, the subscript g represents gas; ρ_g is the air density; u_g is the air velocity; P_g is the air pressure.

The relationship between air wave speed and air density is as follows:

$${c_g}^2 = P_g {\rho_g}^{-1} \tag{5}$$

$$\frac{{c_g}^2}{{c_{g0}}^2} = \frac{{P_g}^{1-\frac{1}{m}}}{{P_{g0}}^{1-\frac{1}{m}}} \tag{6}$$

where, c_g is the air wave speed; m is constant polytropic exponent; c_{g0}, P_{g0} are the initial value of c_g and P_g.

The equation (7) is derived from the joint solution of Equations (5) and (6).

$$\rho_g = k^{-\frac{m}{m-1}} {c_g}^{\frac{2}{m-1}} \tag{7}$$

where k is a constant, $k = \frac{{c_{g0}}^2}{{P_{g0}}^{1-\frac{1}{m}}}$.

Substituting equation (7) into (3) and (4), the following formula can be obtained:

$$\frac{\partial c_g}{\partial t} + u_g \frac{\partial c_g}{\partial x} + \frac{m-1}{2} c_g \frac{\partial u_g}{\partial x} = 0 \tag{8}$$

$$\frac{\partial u_g}{\partial t} + u \frac{\partial u_g}{\partial x} + \frac{2}{m-1} c_g \frac{\partial c_g}{\partial x} = 0 \tag{9}$$

The moving air–water interface during the whole rapid filling process is governed by the continuity and pressure balance equations as:

$$L_w = L_{w0} + \int_0^t V_{interface} dt \tag{10}$$

$$H_w = \frac{P_g}{g\rho_g} + Z_{interface} \tag{11}$$

where L_w is the water length; L_{w0} is the initial value of L_w; $V_{interface}$ is the moving speed of the air–water interface; H_w is the piezometric head at the air–water interface; $Z_{interface}$ is the elevation of the air–water interface.

3. Method of characteristic for discreated air pocket

Accurate numerical simulation methods are essential to understand and mitigate these challenges. In this section, the above mathematical model is rewritten into the form of the method of characteristic (MOC). The ordinary differential form of the water equations is relatively mature, and the partial differential equation transformation of air equation is emphasized here. The MOC has been widely used to simulate two-phase transient flow. Pozos-Estrada (2018) used this method to conduct numerical and experimental studies on the influence of air–water mixed flow patterns. Alexander et al. (2020) used the MOC to study the blocking effect of local air pockets on pipeline transport. Ling Zhou et al. (2011) employed it to develop insights into rapid filling processes with retained air pockets on pipeline pressure.

For a pipe section filled with water, the following equation can be obtained by integrating the positive and negative characteristic lines of the standard one-dimensional unsteady flow:

$$C^+ : H_{wi}^{t+\Delta t} = H_{w(i-1)}^t + \frac{a_w}{gA} Q_{w(i-1)}^t - \left(\frac{a_w}{gA} + \frac{f \Delta x}{2gDA^2} |Q_{w(i-1)}^t| \right) - \frac{J_U \Delta x}{g} \tag{12}$$

$$C^- : H_{wi}^{t+\Delta t} = H_{w(i+1)}^t - \frac{a_w}{gA} Q_{w(i+1)}^t + \left(\frac{a_w}{gA} + \frac{f \Delta x}{2gDA^2} |Q_{w(i+1)}^t| \right) + \frac{J_U \Delta x}{g} \tag{13}$$

where, i represents the position of the current solution node, $t + \Delta t$ is the next solution time, D is the inner diameter of the pipe, and A is the area of the pipeline.

The air momentum and continuity equations – Equations (3) and (4) – constitute a pair of quasi-linear hyperbolic partial differential equations with two dependent variables, velocity u_g and air density ρ_g, and two independent variables, distance x and time t along the pipe, respectively. The MOC is used to transform the equation into ordinary differential equation. The simplified air control equations of motion and continuity are identified from Equations (8) and (9) as L_1 and L_2:

$$L_1 = (c_g)_t + u_g (c_g)_x + \frac{m-1}{2} c_g (u_g)_x = 0 \tag{14}$$

$$L_2 = (u_g)_t + u_g (u_g)_x + \frac{2}{m-1} c_g (c_g)_x = 0 \tag{15}$$

These equations are combined linearly using an unknown multiplier λ:

$$L = \lambda L_1 + L_2 = (u_g)_t + u_g (u_g)_x$$

$$+\frac{2}{m-1}c_g(c_g)_x+\lambda(c_g)_t+\lambda u_g(c_g)_x$$
$$+\lambda\frac{m-1}{2}c_g(u_g)_x \tag{16}$$

Any two real numbers, with different input values will result in two equations represented by the two dependent variables u_g and c_g, which are equivalent in every respect to Equations (14) and (15). Proper selection of two specific values of λ simplifies the Equation (16). In general, the variables u_g and c_g are functions of x and t. If the variable x is a function of t, then:

$$\frac{du_g}{dt}=(u_g)_x\frac{dx}{dt}+(u_g)_t,\quad \frac{dc_g}{dt}=(c_g)_x\frac{dx}{dt}+(c_g)_t \tag{17}$$

It can be demonstrated that if:

$$\frac{dx}{dt}=u_g+\frac{2}{m-1}\frac{1}{\lambda}c_g=u_g+\lambda\frac{m-1}{2}c_g \tag{18}$$

Then Equation (16) becomes an ordinary differential equation:

$$\lambda\frac{dc_g}{dt}+\frac{du_g}{dt}=0 \tag{19}$$

The solution of Equation (19) yields two characteristic values of λ

$$\lambda=\pm\frac{2}{m-1} \tag{20}$$

By substituting these characteristic values into Equation (18), we can obtain:

$$\frac{dx}{dt}=u_g\pm c_g \tag{21}$$

This demonstrates how the wave position changes over time influenced by the wave propagation speed c_g and velocity u_g. Consideration of positive and negative values in Equation (21) together with Equation (17) leads to two pairs of equations which are grouped and identified as C^+ and C^- equations.

$$C^+:\begin{cases}\dfrac{2}{m-1}\dfrac{dc_g}{dt}+\dfrac{du_g}{dt}=0\\ \dfrac{dx}{dt}=u_g+c_g\end{cases}$$
$$C^-:\begin{cases}-\dfrac{2}{m-1}\dfrac{dc_g}{dt}+\dfrac{du_g}{dt}=0\\ \dfrac{dx}{dt}=u_g-c_g\end{cases} \tag{22}$$

Thus two real values of λ have been used to convert the original two partial differential equations to two total differential equations, each with the restriction that they are valid only when the respective conditions are met.

4. Results and discussion

This section assesses the proposed DAM through an experiment system and large scale pipe system. This is to (a) examine the numerical dissipation caused by the solution scheme of the DAM; (b) validate the accuracy of the DAM simulation results by comparing with the experimental data and the results of the UAM; (c) execute a sensitivity analysis of the proposed model and clarify its precision in various applications; (d) investigate the intrinsic mechanism of the model and the wave propagation process. This section uses two systems with the first one being an 8.862-meter experimental system with an upstream air tank (0.08 MPa and 0.12 MPa), a closed downstream end, and initial air lengths of 0.3 m and 0.4 m at atmospheric pressure. The transient in this system is triggered by opening a valve in 0.01 s (see Section 4.1). The second system is a 2400-meter long system with an upstream pressure of 0.392 MPa, a closed downstream end, and initial air at atmospheric pressure. Different air lengths are tested for sensitivity analysis, with the transient also initiated by rapid valve opening at 0.01 s.

4.1. Verification of proposed model

In smooth pipes, the friction interference can be removed, and an adiabatic model is used. The only reason for the pressure attenuation in the pressure curve over time is the numerical dissipation of the solution scheme itself. Figure 1 shows the simulation results of the DAM and the UAM in a smooth rigid pipe, and sets a horizontal line with the first peak point as the reference to visually show the numerical dissipation. In Figure 1, compared with the results of the uniform air model, the simulation results of the discrete air model are almost unaffected by numerical dissipation. The two models have consistent simulation results in the first cycle, and the phase deviation is slightly present in subsequent cycles. This

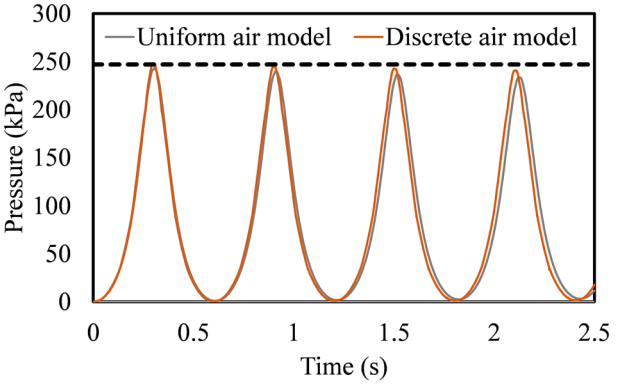

Figure 1. Calculation results of the DAM and UAM in smooth pipe.

difference is due to the introduction of the air governing equation, where the DAM considers the transfer of pressure through each air node, while the UAM assumes that all air nodes have the same response to pressure waves. With the development of time, the dynamic characteristics of air in the DAM can be better reflected and the cumulative error difference over time is shown.

The experiment carried out by Zhou et al. (2023) used an 8.862 m long pipe with a diameter of 0.04 m to verify the numerical model. The experiment's upstream pressurized air tank with constant pressure P_r was connected to the downstream closed end by an 8.862 m length pipe. A valve installed 5.526 m downstream of the tank and was initially completely closed to separate water and air. Air length (L_{a0}) between the valve and downstream closed end is initially atmospheric. Subsequently, the valve was suddenly opened within 0.01s, initiating transient events of rapid filling. For four cases (P_r = 0.08 and 0.12 MPa, L_{a0} = 0.3 and 0.4 m) under the same conditions for both the model and the experiment, Figure 2 presents a comparison between the pressure fluctuation results from the DAM and those from both the UAM and experiments. The comparative analysis was concluded by aligning both models to the four cases' various upstream pressures and air lengths. The analysis shows that both models yield similar simulation results for the first peak pressure. In subsequent cycles, the DAM simulation results are more closely aligned with the experimental data during the subsequent wave period and yields more consistent phase results compared to experimental data when the transient wave from valve opening reaches the air pocket. This is due to the incorporation of an improved air governing equation, which allows for a more accurate representation of wave reflection within the air pocket.

Minor peak differences between the two model's simulations exist in the four cases' system settings, necessitating further exploration of parameter sensitivity. Research by Alexander et al. (2020) and Li et al. (2024) suggest that energy loss from transient wave transport at the air–water interface could be a cause.

Overall, the air reflection characteristics incorporated in the discrete air model create more realistic pressure fluctuations, validating its accuracy in simulating rapid filling transient events.

4.2. Sensitivity analysis of pipeline system applications

Usually, the length and diameter of the experimental pipe differ from those of actual engineering pipe systems due

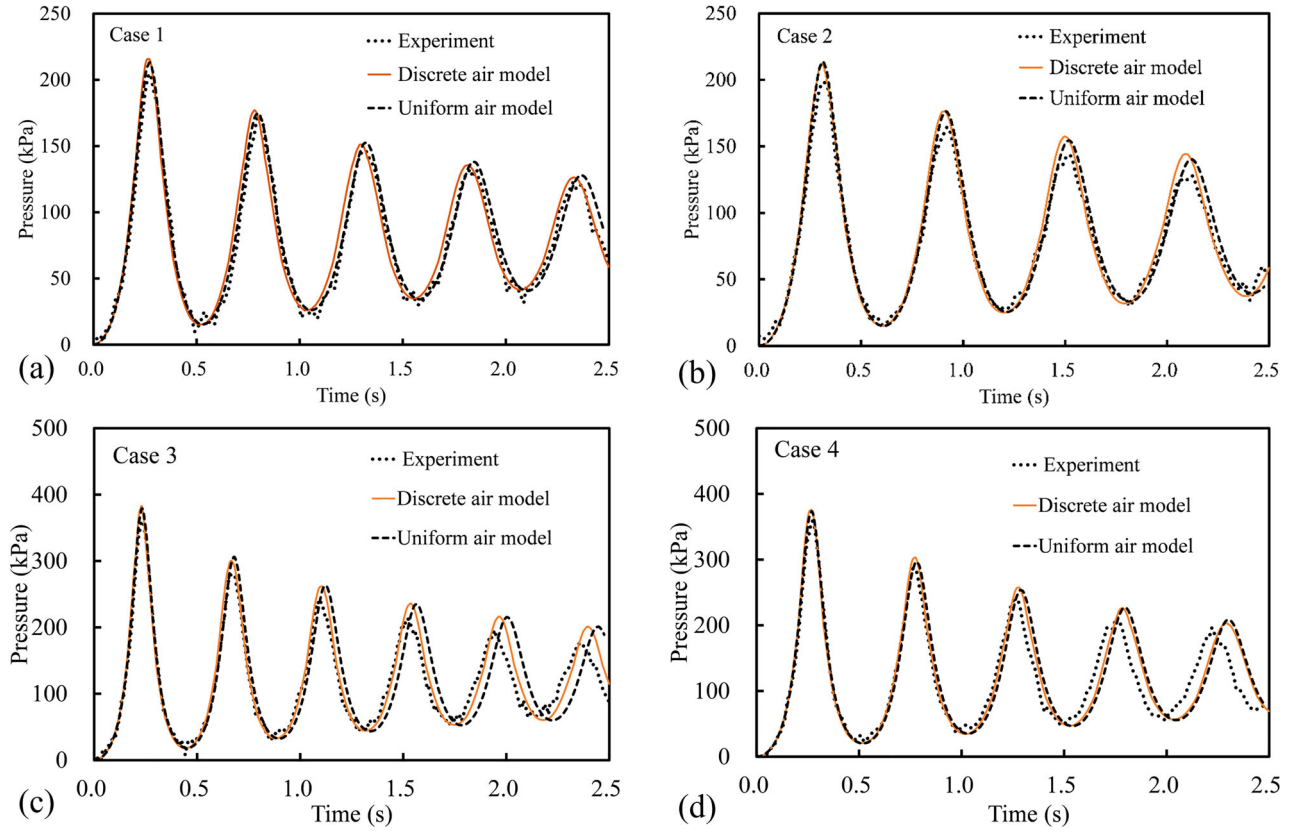

Figure 2. Comparison of DAM, UAM and experimental results (a) Case 1: P_r = 0.08 MPa, L_{a0} = 0.3 m (b) Case 2: P_r = 0.08 MPa, L_{a0} = 0.4 m (c) Case 1: P_r = 0.12 MPa, L_{a0} = 0.3 m (d) Case 1: P_r = 0.12 MPa, L_{a0} = 0.4 m.

to the space and budget constraints during the design of the experimental facility. The purpose of this sub-section is to explore the role of air in practical systems with large-scale pipes, i.e. long pipes with big diameters. Influences of air content, pipe size and other parameters are investigated here.

4.2.1. Analysis influence of initial air length

The influence of different air content on the transient process of the experimental system is shown in Figure 3(a). The experimental system parameters are the same as previously stated with upstream pressure of 0.12 MPa. Air content α refers to the ratio of the air volume in the pipe to the total pipe volume. With increased air content, the difference between the DAM and UAM simulations becomes more significant. The experiment affirms that the DAM with the air governing equation can generate more credible pressure fluctuations, indicating the need for further exploration to investigate the dynamic characteristics of large air content.

To investigate air behaviour via two modelling approaches during the filling process of an engineering large-scale water pipe, a long pipe configuration with an intermediate valve, closely resembling the experimental system was proposed. The total length was 2400 m, with a inner diameter of 0.3 m. The system's upstream inlet pressure was 0.392 MPa and the downstream end of the pipe is closed.

The simulation results of the DAM and UAM with proposed long system at different initial air ratio are illustrated in Figure 3(b), showing that for larger initial air ratio there is no discernible difference between the pressure curves produced by the two models, and for lower initial air content ($\alpha = 3\%$) the UAM presents a slight earlier first peak. Given that, the strength of the DAM lies in its depiction of wave reflection in air, enhancing pressure calculation accuracy. The possible reason for yielding similar results between two models is that the long system is specific and large enough that the peak of the pressure curve is not obvious. In the same pipe system, when the air pocket length is long, it provides a cushioning effect; when the air pocket length is short, instantaneous compression will easily cause the air to produce a large pressure surge. The suitability of the discrete air model needs to be further explored for different pipe parameters systems with the same air content, and it is necessary to determine the specific pipeline conditions in which it can be applied.

4.2.2. Analysis of pipe scale influence

The pipe diameter ratio (β) is defined as the ratio of pipe length to diameter ($\beta = L/D$), which is an intuitive parameter that reflects the influence of pipe scale on transient process. Figure 4(a) presents the simulation results of the two models when the pipe diameter ratio L/D is 2500 and air content is 99.6%. The results indicate that both models produe similar outcomes under different pipe lengths with the same diameter ratio. For the DAM, under the same pipe diameter ratio and initial air content, the longer the pipe, the more obvious the stepped-like rising fluctuation becomes. However, as shown in Figure 4(b), the results of the two models differ significantly when β varies. The DAM, with its superior accuracy validated by experimental data (Figure 2), is chosen as the baseline. As β increases, the deviation of the UAM simulation results becomes smaller.

As shown in Table 1, the deviation in the calculation results for various pipe diameter ratios between the DAM and UAM is quantified. The relative error is used, i.e. the interpolation between the results of the DAM (P_{DAM}) and the UAM (P_{UAM}) divided by P_{DAM} as error $= (P_{\mathrm{DAM}} - P_{\mathrm{UAM}})/P_{\mathrm{DAM}}$. An error threshold of

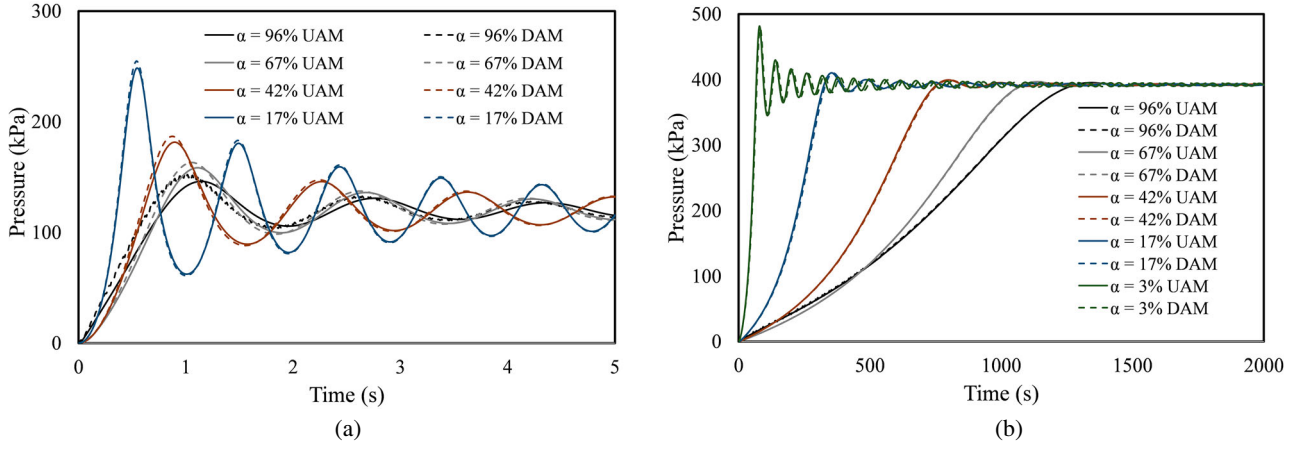

Figure 3. Comparison of simulation results of UAM and DAM at different initial air content (a) experimental system with pipe length of 8.862 m (b) large-scale system with pipe length 2400 m.

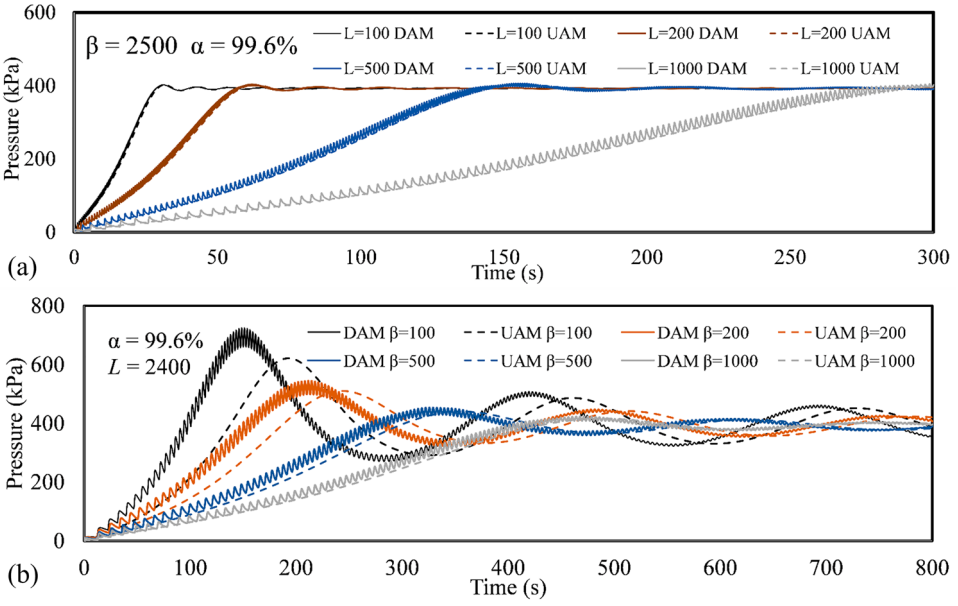

Figure 4. Simulation results of two models with the same initial air content (a) pipe diameter ratio β 2500 (b) different pipe diameter ratio.

Table 1. Simulation results for models with different L/D with pipe length 2400 m and inlet pressure 0.392 Mpa.

β	Maximum pressure of DAM (kPa)	Maximum pressure of UAM (kPa)	Relative error (%)
100	724.91	621.33	14.3
200	544.85	510.15	6.4
500	454.03	440.33	3.0
1000	423.90	416.54	1.7
2000	407.48	404.52	0.7
3000	402.05	400.49	0.4
5000	397.75	397.26	0.1
8000	395.60	395.44	0.0
10000	394.93	394.83	0.0

no more than 1% is used as the standard, and the findings demonstrate that when the pipe diameter ratio of $L/D = 2000$ is used as the threshold, within this limit, the DAM and UAM provide identical results. Beyond this threshold, the UAM begins to show a gradual increase in calculation error, ultimately underestimating the maximum pressure peak. The simulation results of both models are similar when $\beta = 3000$. Conversely, the UAM significantly underestimates peak pressure and delays peak time when $\beta = 200$.

According to the analysis of pipe diameter ratio, the pipe diameter ratio of the experimental system is 221.5, and the simulation results of the discrete air model are more consistent with the experimental data. For the proposed long system, the pipe length is 2400 m and the pipe diameter ratio is 8000, so the simulation results of the two models are very similar. In addition, due to the consideration of air characteristics, the curve rise process of the DAM is accompanied by a stepped waveform. This is because the DAM can effectively capture the accumulation of the pressure wave exchange process at the interface along during the transfer process. Therefore, to further analyze the influence of discrete air, the next analysis is carried out from the perspective of wave speed.

4.3. Transient wave propagation in air

This section focuses on a case to explore the effect of the model taking into account air characteristics on simulation results.

As can be seen in Figure 5, the change in pressure during the water filling process was analyzed using the proposed long system with pipe length of 2400 m. Although

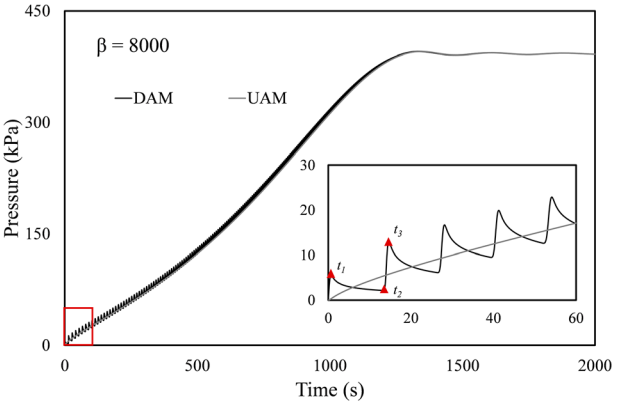

Figure 5. Pressure fluctuation during water filling process in UAM and DAM.

both models yield generally similar simulation results, it is worth noting that the discrete air model provides a more detailed depiction of pressure fluctuations.

At t_1, there is a small jump in pressure caused by the transfer of a transient wave to the interface. Initially, the interface is very close to the upstream, and transient waves arrive very quickly.

Before time t_2, the pressure gradually decreases until it reaches lowest value, at which time the transient wave passes downstream from the interface and returns, and there are constant depressurization waves returning along the way. Since the pressure is always positive, no cavitation occurs. The change in wave speed in the air can more intuitively show the propagation of the transient wave. Figure 6(a)–(c) shows the change in air wave speed along the pipeline over time. The initial air wave velocity is related to air density and pressure, and the initial value is about 322 m/s. Among them, Figure 6(a) shows that the transient wave propagates downstream, Figure 6 (b) shows changes at the downstream boundary, and Figure 6(c) shows the transient wave propagates from the downstream to the interface. When it propagates at the interface of the intersection, the pressure in Figure 5 drops to the local lowest point, which is exactly at time t_2.

At t_3, there is another jump in pressure, caused by the transient wave returning to the interface. Corresponding to Figure 6(d), after the wave speed change at the interface is completed, the pressure reaches the highest local point.

Subsequent fluctuation repeats this process continually. As the interface advances forward, the overall trend of pressure increases. Figure 7(a) shows the interface's advancement over time through the change in air wave speed.

Wave propagation speed in water is approximately 1000 m/s, while in air it is slower at around 322 m/s, which helps to determine the interface location based on the difference in wave speed between the two phases. In addition, during the filling process, the air's pressure characteristic after compression is shown in Figure 7(a). As seen from Equation (5), the wave speed of the air is proportional to the pressure, and the gradual increase in wave speed reflects the pressure characteristic of the air.

Figure 7(b) shows the temperature change along the pipe. Due to the large specific heat capacity of water, the temperature changes only slightly in the water section, while the temperature changes in air are more significant. The temperature change during this process is consistent with the pressure wave propagation process. The air temperature shows an upward trend during filling process,

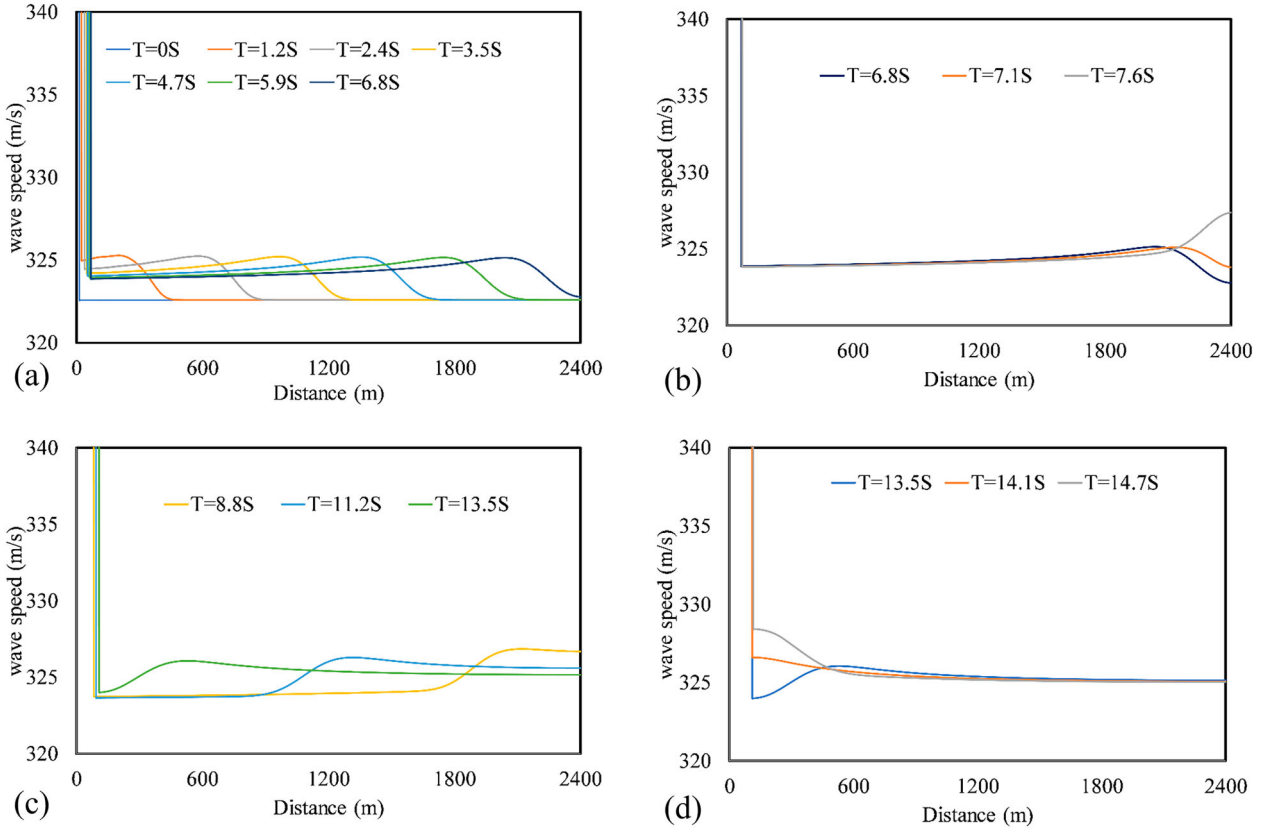

Figure 6. Wave speed propagation along the pipe at different times. (a) Wave speed transfer to the end (b) terminal wave speed change (c) wave speed transfer to the interface (d) interface wave speed change.

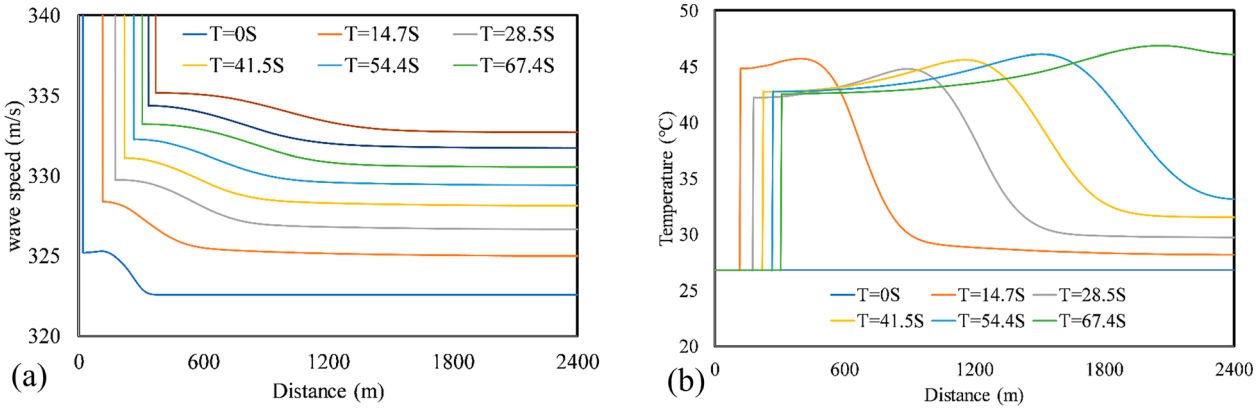

Figure 7. Continuous propagation of wave speed with interface propulsion (a) Wave speed (b) temperature change.

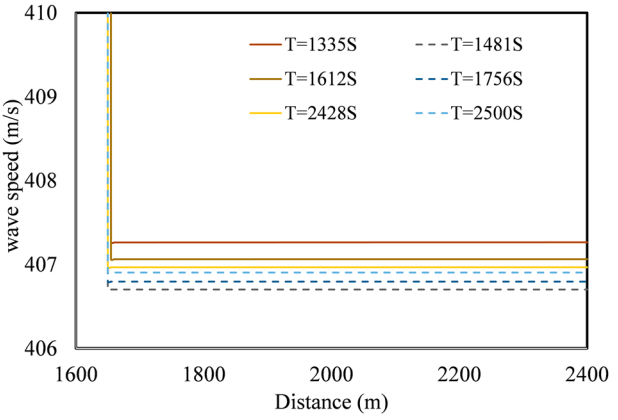

Figure 8. Reaching stable after some fluctuations.

increasing by about 20°, reaching around 45°, though the rise is not very obvious. The formula for calculating temperature change (Te) is as follows:

$$Te = \frac{P_g L_g \pi D^2}{4 M_g R_g} \tag{23}$$

where, L_g is the air length; M_g is the air mass; R_g is air constant.

Figure 8 shows that after the pressure reaches its maximum, it stabilizes after several small fluctuations. These pressure fluctuations occur due to the compression-expansion characteristics of the air. At this point, the position of the interface moves very little, and the fluctuation in wave speed reflects the fluctuation in pressure.

In general, the characteristics of the transient wave in the filling process can be divided into three stages: (1) propagation stage in the pipe with multiple variations, as shown in Figure 6; (2) maximum value stage with the interface advancing, as shown in Figure 7; (3) stability stage after several fluctuation of system, as shown in Figure 8.

Table 2. The increased rate of wave speed at interface with different diameter ratio with pipe length 2400 m and inlet pressure 0.392 MPa.

β	a_2 (m/s)	t_2 (s)	a_3 (m/s)	t_3 (s)	γ
100	328.18	11.53	341.09	14.12	4.98
200	326.91	11.88	338.80	14.29	4.93
500	325.49	12.12	335.86	14.35	4.65
1000	324.75	12.41	333.80	14.47	4.39
2000	324.25	12.53	331.85	14.53	3.80
3000	324.02	12.59	330.76	14.59	3.37
5000	323.78	12.65	329.46	14.65	2.84
8000	323.59	12.82	328.40	14.76	2.50
10000	323.51	13	327.93	14.82	2.43

t_2, t_3 is the time shown in Figure 5.
a_2, a_3 is the corresponding wave speed at t_2 and t_3 and is also the local minimum and maximum wave speed.

Since the important process of wave propagation in the air pocket is given, and the relationship between pressure fluctuation and wave propagation is explained in detail, the influence of the pipe diameter ratio (β) on the results of the discrete air model can be explained from the perspective of the change of air wave speed. The increased rate of wave speed (γ) is defined as the rate at which the wave speed changes at the air–water interface and it is calculated by the difference of wave speeds a_2 and a_3, which is corresponding to the start time t_2 and the end time t_3 at which the interface is affected by a transient wave divided by the time difference, i.e. $\gamma = (a_2 - a_3)/(t_2 - t_3)$.

The change of γ under different pipe diameter ratios (β) is shown in Table 2.

Table 2 shows that the pipe system with a smaller diameter ratio has a larger wave speed growth rate at the interface, which means that the first stage of transient wave propagation in the filling process will result in a larger pressure step rise. This process is taken into account in DAM by incorporating air characteristics, making the simulation results more accurate and clarifying why the results of the two models are biased in systems with large diameter ratios.

5. Conclusions

This paper addresses a key knowledge gap regarding appropriate methods for incorporating pressurized air characteristics into water-filled system modelling for mathematical model development. The discrete air model (DAM) was constructed and compared against two standards: the uniform air model (UAM) and experimental results. This approach allowed an assessment of the accuracy of the proposed model. Finally, the model is applied to large-scale engineering pipelines to investigate the dynamic characteristics of air. Key findings of this research are presented as follows:

(1) The model's accuracy is demonstrated by comparing the results of the DAM with those of both the original UAM and experimental data.
(2) The parameter sensitivity of the DAM is analyzed. The main factors are the initial air content α and the system pipe diameter ratio β. The simulation results are compared with those of the UAM. It is shown that there is a critical value of pipe diameter ratio ($\beta = 2000$). Below this value, the simulation results of the two models diverge, with the UAM tending to underestimate the maximum pressure generated.
(3) The propagation process of transient waves is presented, highlighting three distinct propagation stages: the propagation stage with multiple repeats, the maximum value stage, and the stability stage after several fluctuations. These stages illustrate the propagation of transient waves in the filling process from the perspective of air wave speed changes.
(4) The inceased rate of wave speed (γ) at the air–water interface plays a pivotal role during the filling process, with the discrete air providing more accurate pressure change results when the diameter ratio is less than the threshold value.

The application of the proposed DAM to large-scale water pipelines, following its verification, offers a valuable reference for exploring the scale effect of air propagation in long-distance and large pipe diameter scenarios. Additionally, based on the research presented in this paper, a large-scale experimental system for long-distance water pipeline could be established in the future, allowing for a deeper study and verification the dynamic characteristics of air pockets in large-scale pipeline systems. This would aid in developing and refining a more effective model for rapid water filling at the real air–water interface, thereby enriching the corresponding theoretical and numerical analysis.

Disclosure statement

No potential conflict of interest was reported by the author(s).

Funding

This work was supported by the National Natural Science Foundation of China [grant numbers 51679066 and 51839008], the China Scholarship Council [file number 202306710100] and the European Commission [grant number 101008626].

Data availability statements

The data collected during the study are available from the corresponding author by request.

Nomenclature

H_w	the piezometric head, m;
V_w	the average flow velocity of the pipe cross section, m/s;
a_w	the wave speed, m/s;
D	pipe diameter, m;
J_Q	loss terms due to steady friction;
J_U	loss terms due to unsteady friction;
G	acceleration of gravity, m/s^2;
X	distance along pipe, m;
Δx	unit mesh length;
T	current computation time, s;
ρ_g	the air density, kg/m^3;
u_g	the air velocity, m/s;
P_g,	the air pressure and the initial value of the air pressure, Pa;
c_g, c_{g0}	the air wave speed and its initial value, m/s;
M	constant polytropic exponent;
L_w, L_{w0}	the water length and the initial value of water length, m;
$V_{interface}$	the moving speed of the air–water interface, m/s;
$Z_{interface}$	the elevation of the air–water interface, m;
H_w	the piezometric head at the air–water interface, m;
Q_w	water flow rate, m^3/s;
L_1, L_2	the representation of motion and continuity equation of air;
K	intermediate parameter;
i	the position of the current solution node;
A	the area of the pipeline, m^2;
λ	unknown multiplier;
F	friction coefficient.

Subscripts

g	gas phase
w	water phase

Q	steady friction
U	unsteady friction
i	the position of the solution node
interface	air–water interface

Abbreviations

DAM	Discrete air model
UAM	Uniform air model

References

Alexander, J. M., Lee, P. J., Davidson, M., Li, Z., Murch, R., Duan, H. F., & Brunone, B. (2020). Experimental investigation of the interaction of fluid transients with an in-line air pocket. *Journal of Hydraulic Engineering*, *146*(3), 04019067. https://doi.org/10.1061/(ASCE)HY.1943-7900.0001691

Besharat, M., Coronado-Hernández, O. E., Fuertes-Miquel, V. S., Viseu, M. T., & Ramos, H. M. (2018). Backflow air and pressure analysis in emptying a pipeline containing an entrapped air pocket. *Urban Water Journal*, *15*(8), 769–779. https://doi.org/10.1080/1573062X.2018.1540711

Bucur, D. M., Dunca, G., & Cervantes, M. (2017). Maximum pressure evaluation during expulsion of entrapped air from pressurized pipelines. *Journal of Applied Fluid Mechanics*, *10*(1), 11–20. https://doi.org/10.18869/acadpub.jafm.73.238.26313

Chaiko, M. A., & Brinckman, K. W. (2002). Models for analysis of water hammer in piping with entrapped air. *Journal of Fluids Engineering*, *124*(1), 194–204. https://doi.org/10.1115/1.1430668

City of Edmonton. (1995). *Report on the July 4, 1995 storm event*. Drainage Branch, Transportation Department, City of Edmonton, Edmonton, Alta.

Coronado-Hernández, O. E., Fuertes-Miquel, V. S., Iglesias Rey, P. L., & Martínez-Solano, F. J. (2018). Rigid water column model for simulating the emptying process in a pipeline using pressurized air. *Journal of Hydraulic Engineering*, *144*(4), 1–7. https://doi.org/10.1061/(ASCE)HY.1943-7900.0001446

Ferreira, J. P., Ferràs, D., Covas, D. I., van der Werf, J. A., & Kapelan, Z. (2024). Air entrapment modelling during pipe filling based on SWMM. *Journal of Hydraulic Research*, *62*(1), 39–57. https://doi.org/10.1080/00221686.2024.2305354

Fuertes-Miquel, V. S., Coronado-Hernández, O. E., Mora-Meliá, D., & Iglesias-Rey, P. L. (2019). Hydraulic modeling during filling and emptying processes in pressurized pipelines: A literature review. *Urban Water Journal*, *16*(4), 299–311. https://doi.org/10.1080/1573062X.2019.1669188

Fuertes, V. S., Arregui, F., Cabrera, E., & Iglesias, P. L. (2000). Experimental setup of entrapped air pockets model validation. *BHR Group Conference Series Publication*, *39*, 133–146.

Hamam, M. A., & McCorquodale, J. A. (1982). Transient conditions in the transition from gravity to surcharged sewer flow. *Canadian Journal of Civil Engineering*, *9*(2), 189–196. https://doi.org/10.1139/l82-022

Hatcher, T. M., & Vasconcelos, J. G. (2017). Peak pressure surges and pressure damping following sudden air pocket compression. *Journal of Hydraulic Engineering*, *143*(4), 04016094. https://doi.org/10.1061/(ASCE)HY.1943-7900.0001251

Hou, Q., Li, S., Tijsseling, A. S., & Laanearu, J. (2020). Discussion of 'rigid water column model for simulating the emptying process in a pipeline using pressurized air' by Oscar E. Coronado-Hernandez, Vicente S.Fuertes-Miquel, Pedro L. Iglesias-Rey, and Francisco J. Martinez-Solano. *Journal of Hydraulic Engineering*, *146*(3), 07020001.

Hu, Y., Zhou, L., Li, Y., Lu, Y., Feng, R., Chen, Q., & Xue, Z. (2024). Numerical simulation of various flow regimes in water delivery systems. *Engineering Applications of Computational Fluid Mechanics*, *18*(1), 2387047. https://doi.org/10.1080/19942060.2024.2387047

Li, Y. J., Zhou, L., Li, Z., Che, T. C., Lee, P. J., Lu, Y. Q., & Hu, Y. Y. (2024). Dynamic behaviour and energy dissipation of offline air pockets in transient pipe flows. *Engineering Applications of Computational Fluid Mechanics*, *18*(1), 2387060. https://doi.org/10.1080/19942060.2024.2387060

Lu, Y. Q., Zhou, L., Che, T. C., Xue, Z. J., Li, Y. J., & Hu, Y. Y. (2024). Godunov-type solutions for gas-liquid two-phase transient flows with gas release effects. *Journal of Hydrodynamics*, *35*(6), 1179–1190.

Malekpour, A., & Karney, B. W. (2011). Rapid filling analysis of pipelines with undulating profiles by the method of characteristics. *International Scholarly Research Notices*, *2011*(1), 930460. https://doi.org/10.5402/2011/930460

Mariño, M. A., & Loaiciga, H. A. (1985). Quadratic model for reservoir management: Application to the central valley project. *Water Resources Research*, *21*(5), 631–641. https://doi.org/10.1029/WR021i005p00631

Martin, C. S. (1976). Entrapped air in pipelines. In: *Proceedings of the second international conference on pressure surges, 22–24 September 1976*. BHRA Fluid Engineering.

Pozos-Estrada, O. (2018). Investigation of the combined effect of air pockets and air bubbles on fluid transients. *Journal of Hydroinformatics*, *20*(2), 376–392. https://doi.org/10.2166/hydro.2017.018

Tasca, E., Besharat, M., Ramos, H. M., Luvizotto Jr, E., Karney, B., et al. (2023). Contribution of air management to the energy efficiency of water pipelines. *Sustainability*, *15*(5), 3875. https://doi.org/10.3390/su15053875

Trindade, B. C., & Vasconcelos, J. G. (2011). Numerical simulation of water pipeline filling events with limited ventilation. In *World Environmental and Water Resources Congress 2011: Bearing Knowledge for Sustainability* (pp. 3459–3468). https://doi.org/10.1061/41173(414)363.

Urbanowicz, K., Bergant, A., Stosiak, M., Deptuła, A., & Karpenko, M. (2023). Navier-Stokes solutions for accelerating pipe flow – A review of analytical models. *Energies*, *16*(3), 1407. https://doi.org/10.3390/en16031407

Vasconcelos, J. G., Klaver, P. R., & Lautenbach, D. J. (2015). Flow regime transition simulation incorporating entrapped air pocket effects. *Urban Water Journal*, *12*(6), 488–501. https://doi.org/10.1080/1573062X.2014.881892

Vasconcelos, J. G., & Marwell, D. T. (2011). Innovative simulation of unsteady low-pressure flows in water mains. *Journal of Hydraulic Engineering*, *137*(11), 1490–1499. https://doi.org/10.1061/(ASCE)HY.1943-7900.0000440

Vasconcelos, J. G., & Trindade, B. C. (2011). Discretized air phase modeling in the simulation of pipeline refilling operations. *On modeling urban water systems, monograph 20*. ISBN 978-0-9808853-7-8.

Wylie, E. B., Streeter, V. L., & Suo, L. (1993). *Fluid transient in systems*. Prentice Hall.

Xue, Z., Zhou, L., Liu, D., & Che, T. C. (2023). A random choice scheme for transient mixed flows. *Journal of Hydraulic Engineering*, *149*(8), 04023026. https://doi.org/10.1061/JHEND8.HYENG-13605

Zhou, L., Chen, Q. X., Li, Y. J., Feng, R. L., & Xue, Z. J. (2024). Godunov-type scheme for air–water transient pipe flow considering variable heat transfer and laboratorial validation. *Engineering Applications of Computational Fluid Mechanics*, *18*(1), 2370931. https://doi.org/10.1080/19942060.2024.2370931

Zhou, L., Feng, R. L., Pan, T., Li, Y., Liu, D., & Che, T. C. (2023). Coupled second-order GTS-MOC scheme for transient pipe flows with an entrapped air pocket. *Journal of Hydraulic Engineering*, *149*(9), 04023030. https://doi.org/10.1061/JHEND8.HYENG-13468

Zhou, L., Liu, D., & Karney, B. (2013). Investigation of hydraulic transients of two entrapped air pockets in a water pipeline. *Journal of Hydraulic Engineering*, *139*(9), 949–959. https://doi.org/10.1061/(ASCE)HY.1943-7900.0000750

Zhou, L., Liu, D., Karney, B., & Zhang, Q. (2011). Influence of entrapped air pockets on hydraulic transients in water pipelines. *Journal of Hydraulic Engineering*, *137*(12), 1686–1692. doi:10.1061/(ASCE)HY.1943-7900.0000460